Institute of Physics Publishing | Nanotechnology
Nanotechnology 17 (2006) 4379–4383 doi:10.1088/0957-4484/17/17/015

Plasma-nitrided high-k polycrystalline nano-array induced by electron irradiation

A P Huang[1], L Wang[2], J B Xu[2] and Paul K Chu[1,3]

[1] Department of Physics and Materials Science, City University of Hong Kong, Tat Chee Avenue, Kowloon, Hong Kong
[2] Solid State Laboratory of Electronic Engineering Department, The Chinese University of Hong Kong, Shatin, New Territories, Hong Kong

E-mail: paul.chu@cityu.edu.hk

Received 5 June 2006, in final form 8 July 2006
Published 11 August 2006
Online at stacks.iop.org/Nano/17/4379

Abstract
The microstructure of plasma-nitrided high-k ZrO_2 thin films is found to continuously transform and larger size nano-crystals are formed during electron bombardment. Real-time high-resolution transmission electron microscopy (HRTEM) studies show that the plasma-nitrided nano-size particles can self-crystallize and regrow, whereas this phenomenon is not observed in amorphous ZrO_2 without N incorporation. Similar results are observed in plasma-nitrided HfO_2 samples and fine-scale polycrystalline nano-arrays are obtained by electron irradiation. Our results show that incorporation of N is crucial for inducing microstructural evolution as well as polycrystalline nano-array formation in high-k oxide under electron irradiation.

1. Introduction

As the size of silicon devices is scaled down, the thickness of the gate dielectric film must be significantly reduced as well, and consequently the gate leakage current through conventional SiO_2 dielectrics can become very serious. Various kinds of high-k materials such as Zr-based and Hf-based gate dielectrics have been intensively studied in an effort to reduce the leakage current [1, 2]. Recent studies indicate that the oxygen vacancy (V_O) in high-k gate dielectrics plays a crucial role in the electron leakage current and much attention has been paid to the suppression of V_O formation [3]. Incorporation of nitrogen is a widely accepted technique for reducing the leakage current by the deactivation of the V_O related gap states, and nitrogen doping has been reported to drastically reduce leakage current by three to four orders of magnitude [4]. Theoretical studies using first-principle calculations have clarified the effects of nitrogen doping on the electronic states and leakage current characteristics [5, 6]. However, only several per cent of nitrogen can occupy the oxygen vacancy sites, and most of them are in the interstitial sites in nitrogen-doped Hf-based or Zr-based high-k gate dielectrics which can in fact degrade the dielectric properties of the gate dielectrics and hamper further application. It is critical to control the structure of the materials using crystallization treatments that can produce a fine-scale polycrystalline nano-array or alternatively a much larger crystal size [7]. Electron bombardment in high-resolution transmission electron microscopy (HRTEM) is a suitable means to initiate and monitor the phenomenon. Sinclair *et al* have reported self-crystallization of silicon and the corresponding microstructural evolution at the atomic level by *in situ* HRTEM [8]. Wang *et al* studied the order–disorder transition of mineral materials induced by electron or ion irradiation [9]. Besides, chemical changes in some compounds can occur under electron irradiation as reported by Smith *et al* [10]. However, to our knowledge very little work has been conducted to monitor the microstructure evolution and polycrystalline nano-array growth in nitrogen-doped high-k materials in real-time during electron bombardment.

In the work reported here, plasma-nitrided ZrO_2 thin films were fabricated by cathodic arc deposition and the real-time evolution of the microstructure due to electron bombardment was monitored by HRTEM. Our results reveal the regrowth of

[3] Author to whom any correspondence should be addressed.

 © 2006 IOP Publishing Ltd Printed in the UK

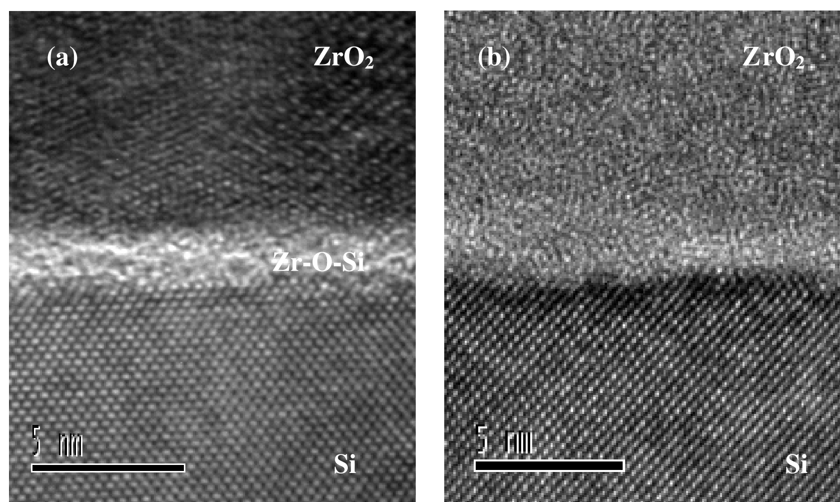

Figure 1. Cross-sectional HRTEM images of ZrO_2 thin films prepared at 450 °C under (a) pure oxygen and (b) oxygen mixed with nitrogen.

plasma-nitrided ZrO_2 nanoparticles and the formation of larger size crystals, whereas this phenomenon is not observed in pure ZrO_2 thin films. Similar results are also observed in plasma-nitrided HfO_2 samples in which a fine-scale polycrystalline nano-array can be obtained by electron irradiation.

2. Experimental details

ZrO_2 thin films with a thickness of 80 nm were fabricated on p-type, 100 mm Si(100) wafers with resistivity of 4–7 Ω cm using plasma nitridation and cathodic arc deposition. The base pressure in the vacuum chamber was about 1×10^{-7} Torr and the substrate temperature was fixed at 450 °C. N_2 and O_2 gases were bled into the vacuum chamber at different flow rates at the vicinity of the metal arc discharge plume to ensure that the gas plasma was simultaneously induced when the cathodic arc was triggered. Plasma-nitrided amorphous HfO_2 thin films of thickness 4 nm were prepared by UHV (ultra high vacuum) electron beam evaporation in conjunction with high concentration ozone oxidation. The *in situ* real-time microstructural evolution of the plasma-nitrided ZrO_2 and HfO_2 samples were monitored using a Tecnai 20 ST, FEG 200 keV HRTEM system of a with an energy resolution of 0.7 eV and an electron beam flux through the sample of about 4×10^{26} electrons m^{-2} s^{-1}. The chemical composition and binding energy of the nitrided and control samples were determined by x-ray photoelectron spectroscopy (XPS) and Rutherford backscattering spectrometry (RBS).

3. Results and discussion

The cross-sectional HRTEM micrographs of the ZrO_2 thin film and nitrided sample are depicted in figures 1(a) and (b). The TEM images show that the ZrO_2 thin film prepared with oxygen has a polycrystalline phase whereas the plasma-nitrided sample is almost amorphous. Moreover, the interfacial layers in the two ZrO_2 samples are obviously different. The former sample shows a 2 nm thick interfacial layer while no visible interlayer can be observed in the nitrided sample. The results suggest that incorporation of nitrogen can increase the crystallization temperature and improve the thermal stability of ZrO_2 thin films. It is believed that plasma nitridation not only impedes crystallization but also effectively blocks oxygen diffusion through the grain boundaries subsequently mitigating the formation of the low-k interfacial layer. In fact, crystallization is a diffusion-limited phase transition driven by the free-energy difference of the phases. Its rate depends on two factors, the free energy difference and the diffusion rate. Nitrogen doping reduces the diffusion rates of all the species and so can inhibit crystallization in the gate dielectric oxides and it has been confirmed employing first-principle calculations [5].

During our TEM observations, the microstructure is seen to continuously transform and the nanoparticles in the plasma-nitrided sample undergo self-crystallization and regrowth. A series of micrographs taken from the same region at 10 s intervals are displayed in figures 2(a)–(d) to illustrate the sequence of the growing ZrO_2 crystallites and formation of large crystals. The initial recording time is t_0 which corresponds to that of figure 2(a) and the following real-time recordings are at (t_0 + 10 s) as indicated in figure 2(b), (t_0 + 20 s) in figure 2(c) and (t_0 + 30 s) in figure 2(d), respectively. The time t_0 represents the time at which the HRTEM observation begins after electron beam focusing that takes less than 3 s. Initially, the nitrided sample mainly consists of the amorphous matrix containing the tetragonal crystalline particles as shown in figure 2(a). It is in good agreement with the spacing of about 0.3 nm between the (101) planes of the tetragonal phase of ZrO_2. The areas labelled A and B are mainly amorphous and no noticeable crystalline particles can be observed. An amorphous matrix surrounding the crystalline particles can be seen in the area (indicated by an arrow) in figure 2(a). With increasing electron irradiation time, the nanoparticles undergo real-time regrowth, and self-crystallization is clearly observed in figure 2(b). As more time elapses, the initial amorphous areas in figure 2(a) gradually disappear whereas the crystalline nanoparticles grow larger, as shown in figure 2(c), especially in the areas labelled A and B. After more electron beam irradiation, some dislocations in

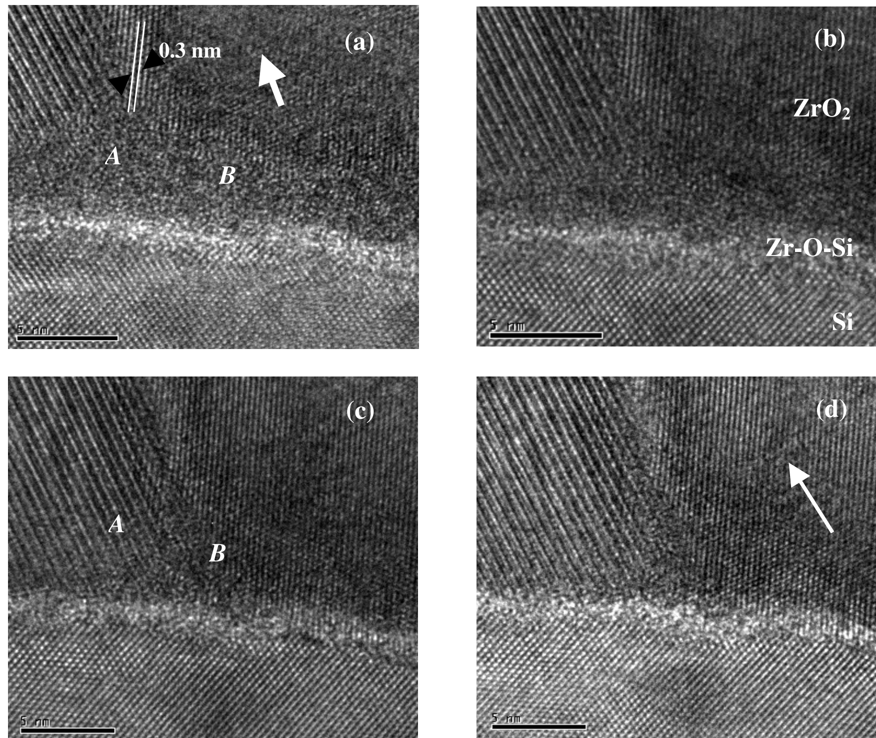

Figure 2. Real-time HRTEM micrographs taken from the plasma-nitrided ZrO_2 sample after different periods of electron bombardment: (a) t_0, (b) $t_0 + 10$ s, (c) $t_0 + 20$ s and (d) $t_0 + 30$ s.

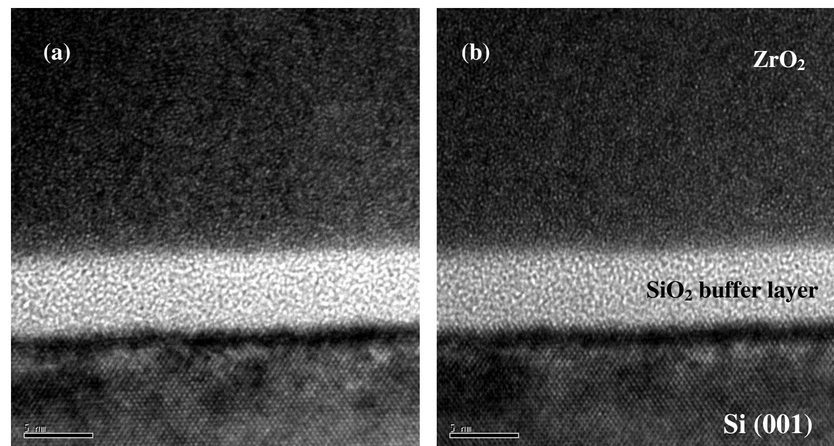

Figure 3. Real-time HRTEM micrographs taken from the pure amorphous ZrO_2 sample at (a) t_0 and (b) $t_0 + 20$ s.

the crystalline particles emerge, as shown in figure 2(d). They may result from the escape of the particles with negative charge such as N induced by long-time irradiation [11]. It is known that electron irradiation, in contrast to thermal annealing or laser illumination, can lead to a different type of crystallization mechanism in which the energy is highly localized both in space (nanometres) and time (picoseconds). Min *et al* have compared the growth rate of high-k Ta_2O_5 thin film without nitridation in an electron beam irradiated area with that of an unexposed area to evaluate the effects of beam exposure and found that the differences are negligible [7]. Sinclair *et al* have reported that the influence of the electron beam may typically amount to a 20 K rise in the local temperature for solid phase epitaxial regrowth of Si [8]. For comparison, the ZrO_2 sample without plasma nitridation fabricated by cathodic arc deposition on a Si wafer with a 5 nm SiO_2 buffer layer in order to obtain the pure amorphous phase was characterized by *in situ* TEM at the same conditions and no obvious change in the microstructure could be found. The images are shown in figures 3(a) and (b), respectively. Our results unequivocally indicate that plasma nitridation is a necessary condition for inducing regrowth and the formation of larger crystals under electron beam irradiation.

In order to further fathom the mechanism of the regrowth of nanoparticles under electron irradiation, plasma-nitrided amorphous HfO_2 ultra-thin films were also prepared on a

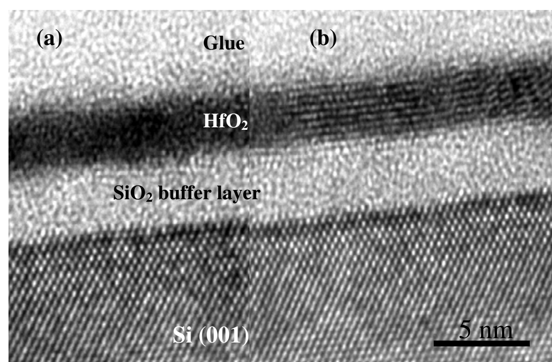

Figure 4. Real-time HRTEM micrographs obtained from the plasma-nitrided HfO_2 sample at (a) t_0 and (b) $t_0 + 20$ s.

silicon wafer with a 5 nm SiO_2 buffer layer by UHV electron beam evaporation. The microstructure is observed by TEM under the same conditions, and the results are shown in figures 4(a) and (b) at t_0 and (t_0 + 20 s), respectively. Although the plasma-nitrided HfO_2 film in figure 4(a) appears to be completely amorphous, the micrograph in figure 4(b) taken from the same region after 20 s of electron irradiation shows that the film is crystallized across a large distance along the film (>1 μm) and a HfO_2 polycrystalline nano-array is formed. This phenomenon is again not observed in the amorphous HfO_2 sample without nitridation (images not shown). Nitrogen doping thus leads to similar effects in Zr-based and Hf-based amorphous gate dielectrics. According to previous reports, nitrogen doping in high-*k* gate dielectrics can greatly suppress film crystallization [3, 5, 6]. Shang *et al* have proposed that substitutional nitrogen can inhibit the crystallization of Hf, Zr and La oxynitrides and improve the thermal stability by reducing the mean atomic coordination [5]. This is because a lower coordination number means fewer constraints per site, and thus it is more likely to be a better glass former. Based on XPS and RBS results, the nitrogen content in our plasma-nitrided samples amounts to nearly 3% and most of them are in the interstitial sites which may break the periodic crystal arrangement or inhibit crystal growth in the gate dielectrics. Figure 5 depicts the N_{1s} core level XPS spectrum of the plasma-nitrided HfO_2 sample, showing two apparent peaks at around 397 and 401 eV. It has been reported by Saha *et al* that the N_{1s} XPS peak at 397 eV arises from atomic β-N for substitutional nitrogen and those at 401 and 402 eV are molecular chemisorbed N–N or N–O for interstitial nitrogen [12]. Furthermore, the peak intensity around 401 eV is obviously stronger than that of 397 eV, suggesting that the nitrogen atoms are mostly located at interstitial sites in the nitrided samples. Under electron beam irradiation, the amorphous atoms or ions can obtain the energy which may arise from the greater activation of pre-existing embryos leading to faster nucleation due to higher atomic mobility. Meanwhile, since the electron beam can penetrate the sample, it can induce the escape of the dissociated nitrogen in the interstitial sites thereby reducing the inhibiting effects on the periodic arrangement of the crystal growth. Wang *et al* have also observed mass losses in nuclear waste glass by electron irradiation and the formation of particulate structures after further irradiation [13].

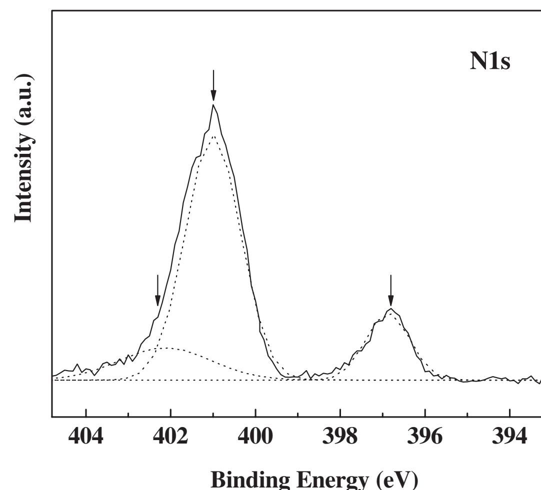

Figure 5. N_{1s} core level XPS spectrum of the plasma-nitrided HfO_2 sample.

Here, although the bonding is predominantly ionic rather than covalent, the ideas about the stability of the amorphous phase of covalent networks are still applicable to high-*k* oxides [5]. The change in the local chemical states, such as a few nearest neighbour exchanges among equivalent sites, can cause breakage of chemical bonds and changes in the valence state of the substitutional nitrogen under electron irradiation, altering their mean atomic coordination and eventually leading to the microstructural transformation. Thus, it is feasible to obtain the plasma-nitrided high-*k* polycrystalline nano-array by electron irradiation.

4. Conclusion

Plasma-nitrided high-*k* ZrO_2 nanoparticles can regrow and larger nano-crystals can be formed by electron bombardment. Similar results are also observed in plasma-nitrided HfO_2 samples in which a fine-scale polycrystalline nano-array can be obtained by electron irradiation. It is worth pointing out that these plasma-nitrided polycrystalline nano-arrays can be used in Si-based devices and will extend the applications of high-*k* gate dielectrics. Further work is under way to study the relative properties of these nano-arrays and the possibility of applying them to CMOS devices.

Acknowledgments

Our work was supported by City University of Hong Kong Strategic Research Grant no 7001981. The authors would like to thank Dr N Ke for technical assistance in the TEM measurements.

References

[1] Aoki Y and Kunitake T 2004 *Adv. Mater.* **16** 118
[2] Wang L, Xue K, Xu J B, Huang A P and Chu P K 2006 *Appl. Phys. Lett.* **88** 072903
[3] Umezawa N, Shiraishi K, Ohna T, Watanabe H, Chikyow T, Torii K, Yamabe K, Yamada K, Kitajima H and Arikado T 2005 *Appl. Phys. Lett.* **86** 143507

[4] Zhu L Q, Zhang L D, Li G H, He G, Liu M and Fang Q 2006 *Appl. Phys. Lett.* **88** 232901

[5] Shang G, Peacock P W and Robertson J 2004 *Appl. Phys. Lett.* **84** 106

[6] Momida H, Hamada T, Yamamoto T, Uda T, Umezawa N, Chikyow T, Shiraishi K and Ohno T 2006 *Appl. Phys. Lett.* **88** 112903

[7] Min K H, Sinclair R, Park I S, Kim S T and Chung U I 2005 *Phil. Mag.* **85** 2049

[8] Sinclair R and Parker M A 1986 *Nature* **322** 531

[9] Lian J, Wang L M, Ewing R C, Yudintsev S V and Stefanovsky S V 2005 *J. Appl. Phys.* **97** 113536

[10] Smith D J, Fryer J R and Camps R A 1986 *Ultramicroscopy* **19** 279

[11] Hu X Y, Cahill D G, Averback R S and Birtcher R C 2003 *J. Appl. Phys.* **93** 165

[12] Saha N C and Tompkins H G 1992 *J. Appl. Phys.* **72** 3072

[13] Sun K, Wang L M, Ewing R C and Weber W J 2005 *Phil. Mag.* **85** 597